

This item is the archived peer-reviewed author-version of:

Electrochemical in situ pH control enables chemical-free full urine nitrification with concomitant nitrate extraction

Reference:

De Paepe Jolien, Clauwaert Peter, Gritti Maria Celeste, Ganigue Ramon, Sas Benedikt, Vlaeminck Siegfried, Rabaey Korneel.- Electrochemical in situ pH control enables chemical-free full urine nitrification with concomitant nitrate extraction
Environmental science and technology / American Chemical Society - ISSN 0013-936X - 55:12(2021), p. 8287-8298
Full text (Publisher's DOI): <https://doi.org/10.1021/ACS.EST.1C00041>
To cite this reference: <https://hdl.handle.net/10067/1797790151162165141>

Electrochemical in situ pH control enables chemical-free full urine nitrification with concomitant nitrate extraction

1 *Jolien De Paepe*^{a,b,c}, *Peter Clauwaert*^{a,c}, *Maria Celeste Gritti*^a, *Ramon Ganigué*^{a,c}, *Benedikt*
2 *Sas*^d, *Siegfried E. Vlaeminck*^{c,e,#} and *Korneel Rabaey*^{a,c,#*}

3 ^a Center for Microbial Ecology and Technology (CMET), Department of Biotechnology,
4 Faculty of Bioscience Engineering – Ghent University, Coupure Links 653, 9000 Gent,
5 Belgium

6 ^b Departament d'Enginyeria Química, Biològica I Ambiental, Escola d'Enginyeria –
7 Universitat Autònoma de Barcelona, Bellaterra 08193 Barcelona, Spain

8 ^c Center for Advanced Process Technology and Urban Resource Efficiency (CAPTURE,
9 www.capture-resources.be)

10 ^d Department of Food Quality and Food Safety, Faculty of Bioscience Engineering – Ghent
11 University, Coupure links 653, 9000 Gent, Belgium

12 ^e Research Group of Sustainable Energy, Air and Water Technology, Department of Bioscience
13 Engineering – University of Antwerp, Groenenborgerlaan 171, 2020 Antwerpen, Belgium

14 # equally contributed as senior authors, * Corresponding author: Korneel.Rabaey@UGent.be

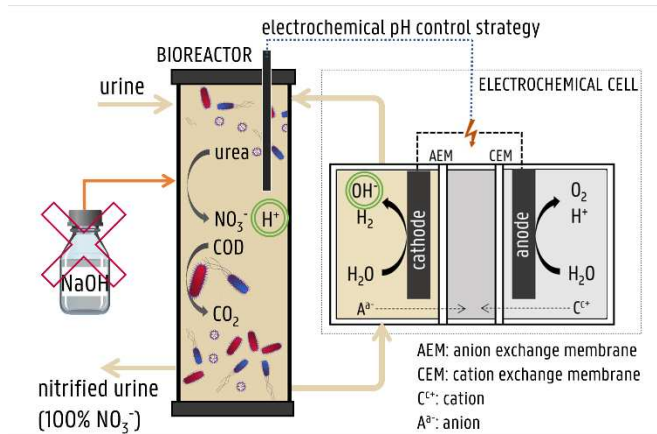
15 **Keywords**

16 Moving bed biofilm reactor; resource recovery; nitrogen recovery; regenerative life support
17 system; MELiSSA

18 **ABSTRACT**

19 Urine is a valuable resource for nutrient recovery. Stabilization is, however, recommended to
20 prevent urea hydrolysis and the associated risk for ammonia volatilization, uncontrolled
21 precipitation and malodor. This can be achieved by alkalization and subsequent biological
22 conversion of urea and ammonia into nitrate (nitrification) and organics into CO₂. Yet, without
23 pH control, the extent of nitrification is limited as a result of insufficient alkalinity. This study
24 explored the feasibility of an integrated electrochemical cell to obtain on-demand hydroxide
25 production through water reduction at the cathode, compensating for the acidification caused
26 by nitritation, thereby enabling full nitrification. To deal with the inherent variability of the
27 urine influent composition and bioprocess, the electrochemical cell was steered via a controller,
28 modulating the current based on the pH in the bioreactor. This provided a reliable and
29 innovative alternative to base addition, enabling full nitrification while avoiding the use of
30 chemicals, the logistics associated with base storage and dosing, and the associated increase in
31 salinity. Moreover, the electrochemical cell could be used as an in situ extraction and
32 concentration technology, yielding an acidic concentrated nitrate-rich stream. The make-up of
33 the end product could be tailored by tweaking the process configuration, offering versatility for
34 applications on Earth and in Space.

35 **TABLE OF CONTENTS (TOC)/ABSTRACT ART**



36

37 **SYNOPSIS**

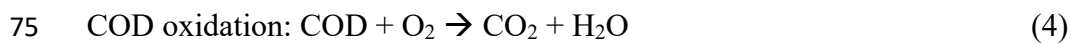
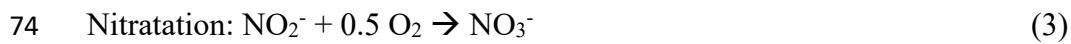
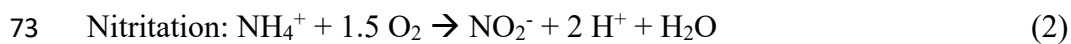
38 This novel, resource-efficient method to transform fresh human urine into a stable and
39 concentrated nutrient solution can contribute to a more sustainable circular nutrient
40 management.

41 1. INTRODUCTION

42 Human urine is a widely available, relatively concentrated source of nitrogen and phosphorus,
43 two essential nutrients in agriculture. Urine source separation at the toilet/urinal allows urine to
44 be collected separately and used as a nutrient resource.¹ The use of urine as a fertilizer or as a
45 raw material for fertilizer production is, however, impeded by the difficulty of collecting the
46 urine and keeping it stable. Urea, the main nitrogen compound in urine, easily and rapidly
47 hydrolyzes to ammonia, ammonium and bicarbonate due to microbial activity, thereby
48 increasing the pH and releasing volatile ammonia, which can be harmful for humans (negative
49 impact on respiratory tract²) and the environment (e.g., toxic, and causing eutrophication and
50 acidification).³⁻⁵ This leads to malodor and uncontrolled precipitation of calcium and
51 magnesium salts and lowers the recovery potential due to nitrogen loss (by ammonia
52 volatilization) and phosphorus loss (by precipitation).⁴⁻⁶ The biofouling potential, caused by the
53 presence of organics in urine which fuel microbial growth, further challenges certain urine
54 treatment technologies (e.g., membrane processes).⁷

55 Urea hydrolysis can be inhibited by increasing the pH immediately after collection, as
56 demonstrated by Randall, et al. (2016)⁸ using $\text{Ca}(\text{OH})_2$, Senecal, et al. (2017)⁹ using a bed of
57 wood ash and De Paepe, et al. (2020)⁶ using a membrane electrolysis cell. The pH increase
58 furthermore triggers precipitation of calcium and magnesium salts, thereby minimizing the risk
59 for downstream scaling and capturing part of the phosphate in precipitates.⁶ Yet, urine is only
60 temporarily stabilized by increasing the pH and still contains urea (which can hydrolyze when
61 the pH is lowered or urease is added⁶) and organics (which can cause biofouling). Treatment in
62 a nitrification-based bioreactor has been reported as a suitable method to biologically stabilize
63 urine^{7, 10-13}, yielding a stable nitrate-rich urine solution low in organics. Urine nitrification
64 requires a well-tuned interplay between heterotrophic and autotrophic bacteria. First, urea is
65 hydrolyzed to total ammonia nitrogen (TAN, i.e., sum of ammonia-N and ammonium-N) by

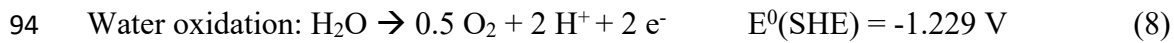
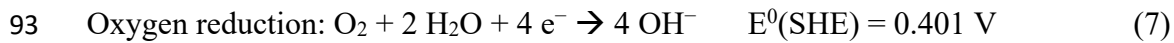
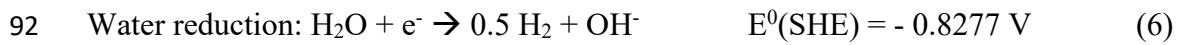
66 urease, an enzyme produced by urease positive (mainly heterotrophic) bacteria (a process
67 commonly referred to as ‘ureolysis’). Subsequently, TAN is oxidized by ammonium oxidizing
68 bacteria (AOB) with oxygen into nitrite (‘nitritation’), which is further oxidized with oxygen
69 into nitrate by nitrite oxidizing bacteria (NOB) (‘nitratation’). Concomitantly, heterotrophic
70 bacteria convert the biologically degradable organics (COD, chemical oxygen demand) into
71 CO₂.



76 Due to the release of protons by nitritation (2 mol H⁺ mol⁻¹ N nitrified) and the limited alkalinity
77 in urine, only about half of the TAN in urine can be converted into nitrate, while the remaining
78 TAN is protonated as non-volatile ammonium due to the acidification, yielding a slightly acidic
79 ammonium nitrate solution.^{11, 14, 15} Full conversion of TAN into nitrate can be achieved by
80 hydroxide addition, typically using a base (e.g., NaOH), and is usually preferred because of the
81 higher process stability (optimal pH and no TAN accumulation) and safety (ammonium nitrate
82 is thermally instable and can be misused as an explosive).^{7, 10, 14} On the other hand, it requires
83 supply, storage of and dealing with hazardous chemicals. Moreover, the increase in salinity
84 resulting from the cation addition (e.g., sodium originating from the use of NaOH) can
85 negatively affect the fertilizer potential of the nitrified urine because many plants are sensitive
86 to high salinities (i.e., the ratio of Na⁺ per N should be limited).^{16, 17}

87 In order to obtain full nitrification while avoiding base addition and the undesirable associated
88 increase in salinity, the bioreactor content is recirculated over the cathodic compartment of an
89 electrochemical cell in this study. Water and/or oxygen reduction at the cathode produces

90 hydroxide ions, which can compensate for the acidification caused by nitritation. At the anode,
91 water is oxidized, producing an acidic stream.



95 To deal with the inherent variability of the urine influent composition and bioprocess, on-
96 demand and automated OH^- production is essential. This can be implemented by controlling
97 the current flow through the electrochemical cell based on the pH in the bioreactor. In-situ
98 electrochemical pH control has already been applied in hydroponic systems^{18,19}, in a bioreactor
99 for continuous culture of yeast cells²⁰, and in fermentation reactors²¹, but has, to the best of our
100 knowledge, not yet been used in combination with nitrification.

101 Nitrified urine can be used as a fertilizer in agriculture (e.g., Aurin, commercial fertilizer
102 produced by VUNA)^{15,22} or as a culture medium for microalgae (e.g., cyanobacteria)^{10,12,23}. In
103 order to reduce the storage and transportation volumes, a concentration step is preferred for
104 terrestrial applications due to the low nutrient concentrations in urine compared to synthetic
105 fertilizers.¹ Interestingly, the electrochemical cell can be used as an in-situ extraction and
106 concentration technology, as demonstrated by Andersen et al. (2015) for a fermentation reactor.
107 Besides countering acidogenic fermentation, the electric field in the electrolysis cell drove
108 carboxylate ions over the anion exchange membrane (AEM) into a cleaner, aqueous
109 concentrated VFA (volatile fatty acids) stream in the latter study.²¹ Similarly, in a nitrification
110 reactor, nitrate migration through an AEM can yield a cleaner, aqueous and concentrated nitrate
111 rich stream.

112 This study aimed to explore the feasibility of an integrated electrochemical cell to dose
113 hydroxide on-demand in a urine nitrification reactor, and to concentrate/refine the produced

114 nitrate. Alkalinized urine (pH 12, to prevent urea hydrolysis in the influent during storage) was
115 fed into a moving bed biofilm reactor (MBBR) which was coupled to an electrochemical cell.
116 Three different configurations were tested at different pH set points and/or concentration
117 factors. To compare the novel electrochemical pH control strategy with base addition and partial
118 nitrification, an identical MBBR with NaOH addition and an MBBR without pH control were
119 operated. All information regarding the operation and the results of these two MBBR are given
120 in the supporting information (SI) Section C and D.

121 2. MATERIALS AND METHODS

122 2.1 Experimental setup

123 An electrochemical cell was installed in the recirculation loop of an MBBR. An MBBR with
124 biofilm carriers was chosen in order to minimize the amount of suspended biomass which could
125 clog the electrochemical cell. The MBBR consisted of a plastic cylinder with an active volume
126 of 3.2 L, of which 24% was filled with polyvinyl alcohol beads (Kuraray Aqua Co, Ltd., Tokyo,
127 Japan), confined in bags made from fine fishnet material and kept in suspension by the aeration
128 and liquid recirculation (SI Figure S1-S2). The reactor was aerated with humidified air using
129 an aquarium pump ($\sim 2\text{-}3\text{ L d}^{-1}$, Air pump 400, Eheim, Germany) connected to diffuser stones
130 installed at the bottom of the reactor. Influent ($\sim 500\text{ mL d}^{-1}$) was dosed using a peristaltic pump
131 and timer, and effluent (and suspended biomass) left the reactor via an overflow at the top of
132 the reactor. The temperature was not controlled and ranged between 20-24°C.

133 The reactor liquid was recirculated from the top to the bottom of the reactor via an external
134 recirculation loop using a peristaltic pump at a flow rate of 18.7 L h^{-1} (5.8 reactor volumes per
135 hour) and passed through the cathodic compartment of the electrochemical cell. The cell was
136 galvanostatically controlled at a current density of $0\text{-}20\text{ A m}^{-2}$ (membrane projected surface)
137 depending on the pH using a programmable power supply (Z+ series, TDK lambda, Japan), a
138 pH probe installed at the outlet of the cathodic compartment (Consort SP10B, Belgium) and a
139 control system programmed in LabVIEW (National Instruments) (SI Section A2). The pH,
140 current and voltage were recorded every 15 seconds.

141 The electrochemical cell consisted of three compartments, made from Perspex® plates and
142 frames with an internal volume of 200 mL ($20 \times 5 \times 2\text{ cm}^3$, anodic and cathodic compartment)
143 or 100 mL ($20 \times 5 \times 1\text{ cm}^3$, middle compartment). A stainless steel wire mesh ($564\text{ }\mu\text{m}$ mesh
144 width, $20 \times 5\text{ cm}^2$, Solana, Belgium) functioned as a cathode and a dimensionally stable titanium

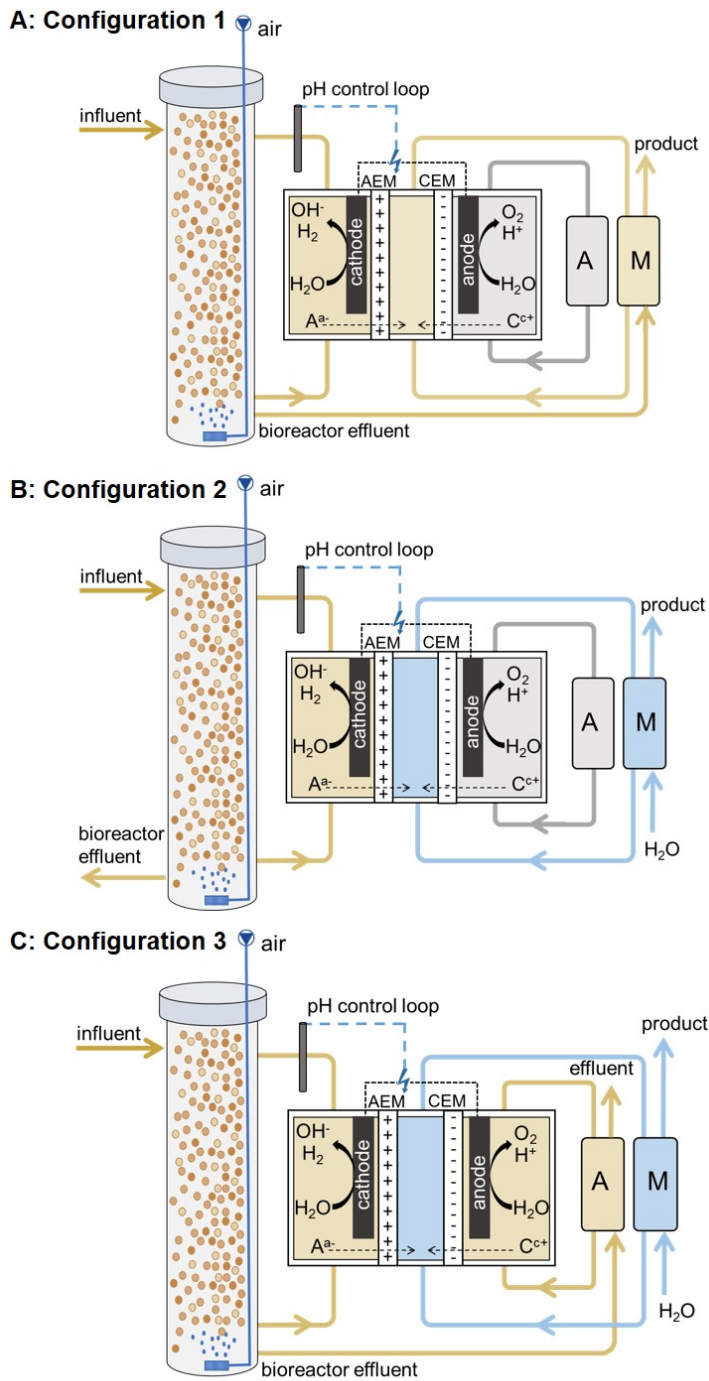
145 electrode coated with iridium MMO (Magneto Special Anodes, The Netherlands) was used as
146 anode. The cathodic and middle compartment were separated by a monovalent AEM (100 cm²,
147 PC MVA PCA GmbH, Germany), whereas a cation exchange membrane (CEM, 100 cm²,
148 Ultrex CMI-7000s, Membranes International Inc., NJ, USA) was installed between the middle
149 compartment and the anodic compartment. Peristaltic pumps were used to recirculate the
150 anolyte and middle compartment solution between the recirculation vessels and electrochemical
151 cell.

152 In configuration 1 (Figure 1A), the aim was to obtain full nitrification and to recover all nitrate.
153 Therefore, the effluent of the bioreactor was pumped from the effluent vessel into the
154 recirculation vessel of the middle compartment using a peristaltic pump (~500 mL d⁻¹) to
155 capture all nitrate that migrated through the AEM. Effluent left the middle compartment
156 recirculation vessel via overpressure. The anodic compartment (initially filled with 0.2 M
157 KH₂PO₄ to minimize the Ohmic resistance) was operated in a closed loop (i.e., without influent
158 or effluent).

159 In configuration 2 (Figure 1B), the goal was to extract and concentrate nitrate in the middle
160 compartment. Demineralised water (~100-225 mL d⁻¹) was fed into the middle compartment
161 recirculation vessel using a peristaltic pump and effluent left the recirculation vessel by
162 overpressure. The anodic compartment (initially filled with 0.1 M Na₂SO₄ to minimize the
163 Ohmic resistance) was again operated in a closed loop.

164 In configuration 3 (Figure 1C), the effluent from the bioreactor was pumped from the effluent
165 vessel into the recirculation vessel of the anodic compartment using a peristaltic pump (~500
166 mL d⁻¹) to enable, besides nitrate recovery, potassium recovery from the urine. The middle
167 compartment was fed with demineralized water (~90 or 180 mL d⁻¹). Effluent left the
168 recirculation vessels via overpressure.

169 **FIGURE 1**



170

171 Figure 1. **Schematic overview of the three configurations.** A: Configuration 1: bioreactor
 172 effluent is fed into the middle compartment. B: Configuration 2: demineralized water is fed into
 173 the middle compartment. C: Configuration 3: bioreactor effluent is fed into the anodic
 174 compartment and demineralized water is fed into the middle compartment. A: anodic
 175 compartment recirculation vessel, M: middle compartment recirculation vessel.

176 **2.2. Urine collection and alkalization**

177 Fresh male urine was collected using a nonwater urinal with approval from the Ethical
178 committee of Ghent University hospital (registration number B670201731862). Immediately
179 after collection, the urine was diluted with water (33.3% urine-66.6% water) simulating the
180 diluting effect of flush water in urine diverting toilets²⁴ and the pH was increased to 12 using a
181 chemical-free electrochemical method developed by De Paepe et al. (2020)⁶ (SI Section A4) in
182 order to prevent urea hydrolysis during storage. Batches of 2-4 L of urine were alkalized with
183 an electrochemical cell, pooled together into large batches of alkalized urine (10-25 L) to
184 average out fluctuations in urine composition in order to provide a stable influent (with a
185 constant composition) to the nitrification bioreactor. The influent batches were stored for up to
186 three months at room temperature. The average influent composition is displayed in SI Table
187 S1. The TAN/TN ratio remained below 5% in the influent of the bioreactor (SI Figure S5),
188 confirming that urea hydrolysis was inhibited by the high pH. Only one batch (used in
189 configuration 2, between day 132 and 136) got contaminated, resulting in a lower influent pH
190 (~9.2) and COD concentration and an increased TAN concentration in the influent (SI Figure
191 S5). This batch was replaced after 5 days. The electrochemical alkalization pre-treatment also
192 reduced the scaling potential by precipitation of divalent cations with phosphate and sulfate.
193 Additionally, the salinity of the urine decreased through the migration of anions (mainly
194 chloride) to the middle compartment. Combined, these two processes resulted in a removal of
195 88 ± 7 % of calcium, 91 ± 6 % of magnesium, 78 ± 16 % of phosphate, 64 ± 14 % of chloride
196 and 58 ± 18 % of sulfate (SI Section A4). The TAN concentration after electrochemical pre-
197 treatment was about 18% lower than before treatment, indicating some ammonia volatilization
198 or ammonia diffusion to the middle compartment. The N loss was however limited as less than
199 5% of the total influent nitrogen was present as TAN.

200

201 2.3 Reactor operation

202 Reactor inoculation and the start-up of the MBBR are described in SI, Section A3. After a start-
203 up of 70 days, the target loading rate was reached (corresponds to ‘day 1’). During the first 13
204 days, the MBBR was operated with regular pH control (i.e., NaOH addition) at a pH set point
205 of 7.5 (Table 1). On day 13, the electrochemical cell was installed in the recirculation loop of
206 the bioreactor and the reactor was operated in configuration 1. Two different pH set points were
207 compared in terms of nitrification efficiency, hydroxide demand and electrode energy
208 consumption. The setup was operated with a pH set point of 7.5 for 43 days and with a pH set
209 point of 6.5 for 27 days. Subsequently, the setup was adapted with the goal to extract and
210 concentrate nitrate in the middle compartment. Configuration 2 was tested with a pH set point
211 of 7.5 at two different influent flow rates to the middle compartment: $\sim 225 \text{ mL d}^{-1}$
212 (corresponding to a $Q_{\text{in bioreactor}}/Q_{\text{in middle compartment}}$ of ~ 2) for 35 days and $\sim 95 \text{ mL d}^{-1}$
213 (concentration factor ~ 5) for 23 days to compare the extraction efficiency, concentration factor
214 and electrode energy consumption. Afterwards, the influent flow rate to the middle
215 compartment was again increased to $\sim 225 \text{ mL d}^{-1}$ (concentration factor ~ 2) for 26 days before
216 changing to configuration 3. Configuration 3 was also tested with two different influent flow
217 rates to the middle compartment: $\sim 180 \text{ mL d}^{-1}$ (between day 168 and day 182) and $\sim 90 \text{ mL d}^{-1}$
218 (between day 182 and day 195).

219 **TABLE 1**

220 **Table 1. Overview of the different operational phases.** Q_{in} =influent flow rate, Q_{out} =effluent
221 flow rate. Average influent and effluent compositions are reported in SI Section B1.

222

	NaOH	Configuration 1		Configuration 2			Configuration 3	
			pH 7.5	pH 6.5	concentration factor 2	concentration factor 5	concentration factor 2	concentration factor 2
Configuration	NaOH control	1	1	2	2	2	3	3
pH set point	7.5	7.5	6.5	7.5	7.5	7.5	7.5	7.5
Concentration factor	1	1	1	2	5	2	2	5
Day	1 - 13	13 - 56	56 - 84	84 - 118	118 - 141	141 - 168	168 - 182	182 - 195
HRT in reactor [d]	6.8 ± 0.2	7.1 ± 0.3	7.1 ± 0.2	6.9 ± 0.3	6.5 ± 0.3	6.8 ± 0.7	7.8 ± 0.7	7.3 ± 0.4
Number of reactor HRT	1.9	6.2	4.1	5.1	3.7	2.6	1.8	1.9
HRT in middle compartment				2.0 ± 0.1	2.6 ± 0.1	2.0 ± 0.3	1.6 ± 0.1	2.5 ± 0.3
Number of HRT in middle compartment				17.2	9.2	17.5	9	5.6
HRT in anodic compartment							1.3 ± 0.1	1.2 ± 0.1
Number of HRT in anodic compartment							11.2	11.8
Q _{in} bioreactor [L d ⁻¹]	488 ± 21	488 ± 22	495 ± 9	501 ± 22	531 ± 24	493 ± 21	447 ± 741	472 ± 24
Q _{out} bioreactor [L d ⁻¹]	502 ± 4 ^b			489 ± 16	511 ± 20	507 ± 4		
Q _{in} middle compartment [L d ⁻¹]				223 ± 16	94 ± 4		180 ± 11	90 ± 5
Q _{out} middle compartment [L d ⁻¹]		484 ± 21	483 ± 11	223 ± 9	119 ± 6		200 ± 10	125 ± 16
Q _{out} anodic compartment [L d ⁻¹]							401 ± 43	423 ± 9
N load [mg N d ⁻¹]	791 ± 42	783 ± 87	716 ± 35	773 ± 23	802 ± 28	796 ± 42	748 ± 74	760 ± 47
N loading rate ^a [mg N L ⁻¹ d ⁻¹]	247 ± 13	277 ± 25	208 ± 10	224 ± 6.5	233 ± 8	252 ± 13	217 ± 21	220 ± 14
COD load [mg COD d ⁻¹]	697 ± 30	676 ± 44	650 ± 36	679 ± 27	538 ± 188	702 ± 30	810 ± 100	753 ± 42
COD loading rate ^a [mg COD L ⁻¹ d ⁻¹]	218 ± 9	196 ± 13	188 ± 10	197 ± 8	156 ± 54	223 ± 9	235 ± 29	218 ± 12

^a volume of 3.2 L in NaOH control or 3.45 L (volume of MBBR and cathodic compartment) in all other phases

^b Effluent flow rate is higher than influent flow rate due to NaOH addition

224 **2.4 Sampling and analytical methods**

225 Samples (10 mL) were taken every 2-3 days, filtered over a 0.22 µm Chromafil® Xtra filter
226 (Macherey-Nagel, PA, USA) and stored in a fridge (4°C) prior to analysis. The samples were
227 brought to room temperature before analysing. The bulk liquid dissolved oxygen (DO)
228 concentration and pH were measured during sampling using a luminescent DO probe
229 (LDO10103, Hach, Belgium) connected to a HQ40d meter (Hach, Belgium) and a portable pH
230 meter (C5010, Consort, Belgium). Ion chromatography was used to determine the concentration
231 of anions (Metrohm 930 equipped with a Metrosep A supp 5-150/4.0 column and conductivity
232 detector, eluent: 1.0 mM NaHCO₃, 3.2 mM Na₂CO₃) and cations (Metrohm 761 equipped with
233 a Metrosep C6-250/4.0 column and conductivity detector, eluent: 1.7 mM HNO₃, 1.7 mM
234 dipicolinic acid). The total nitrogen (TN) and COD concentrations were measured with
235 Nanocolor tube test kits (Nanocolor® TN220 and Nanocolor® COD160/1500, Macherey-
236 Nagel, PA, USA). The electrical conductivity (EC) was measured using a conductivity meter
237 (Consort C6010 with a Metrohm 6.0912.110 conductivity electrode).

238 3. RESULTS AND DISCUSSION

239 3.1. Electrochemical hydroxide production enables full urine nitrification by dynamically 240 compensating for the associated acidification

241 This study aimed to stabilize urine by alkalization and biological conversion of urea and
242 organics into nitrate, CO₂ and biomass. The urine was first alkalized with an electrochemical
243 cell immediately after collection (Section 2.2) to prevent urea hydrolysis during storage, which
244 could reduce the nutrient content and create odor nuisance and scaling. The alkalized urine
245 was then fed into a nitrification MBBR. To enable full nitrification, an electrochemical cell
246 producing OH⁻ through water reduction at the cathode was coupled to the MBBR. The current
247 applied by the power supply was controlled based on the pH of the reactor. At a low pH, a
248 relatively high current was applied to increase the OH⁻ production and, hence, the pH, whereas
249 a high pH in the bioreactor resulted in a lower applied current. After optimizing the settings
250 (i.e., pH set points and corresponding current, SI Section A2) during the first two weeks (day
251 13-26), the pH could be controlled in a narrow range (7.6 ± 0.1) between day 26 and 56 (Figure
252 2A), resulting in full nitrification in the MBBR. The TAN and nitrite concentration in the
253 bioreactor remained below 2 mg N L⁻¹ (Figure 3A). The nitrate concentration in the effluent
254 equalled the total nitrogen concentration in the effluent, indicating that all urea was hydrolyzed
255 and nitrified, but was lower than the total nitrogen concentration in the influent, due to nitrate
256 migration over the AEM (Section 3.2). On average 0.055 ± 0.023 A was applied, supplying 101
257 mmol OH⁻ L⁻¹ to the reactor (assuming a coulombic efficiency of 100%). Together with the
258 hydroxide added during the electrochemical alkalization pre-treatment (~ 29 mmol OH⁻ L⁻¹),
259 a total of 130 mmol OH⁻ L⁻¹ was added which was slightly higher than the theoretical hydroxide
260 demand for full nitrification (SI Table S6).

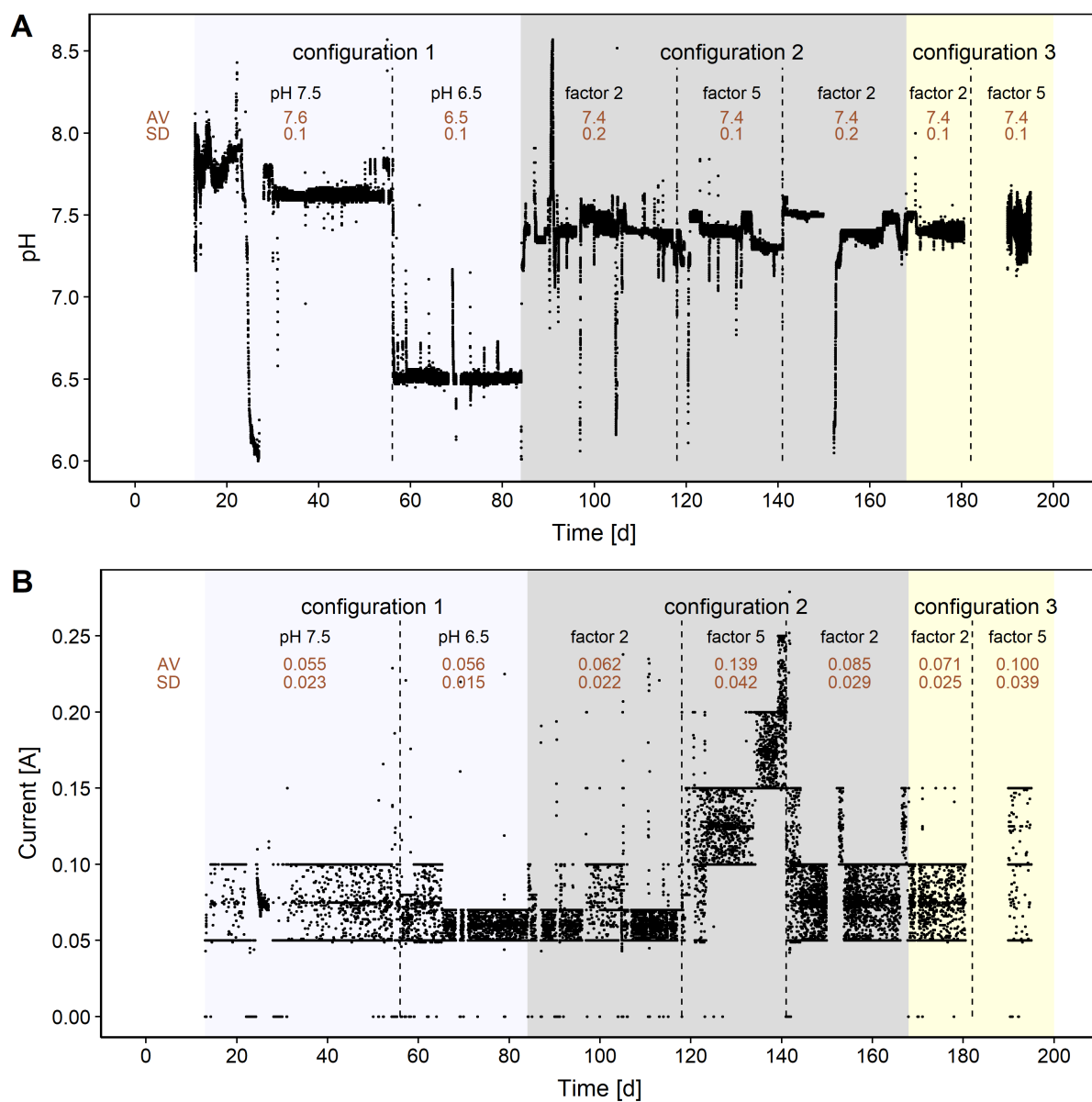
261 To investigate whether a lower pH set point would result in a lower current and thus reduce the
262 energy consumption, the MBBR was controlled at a pH of 6.5 ± 0.1 between day 56 and 84.
263 All urea and TAN were converted into nitrate (Figure 3A), but the average current ($0.056 \pm$
264 0.015) was indifferent from the current at a pH set point of 7.5 (Figure 2B). Titration curves of
265 the middle compartment effluent (SI Figure S8) revealed that only a small increment of 3-5
266 $\text{mmol OH}^- \text{L}^{-1}$ was required to increase the pH from 6.5 to 7.5, which is low compared to the
267 total of $\sim 130 \text{ mmol OH}^- \text{L}^{-1}$ added. This explains the similar current at both pH set points.
268 Hence, lowering the pH set point did not have a significant impact on the energy consumption,
269 but it might affect the nitrification rate. This was observed in the control MBBR with NaOH
270 addition, where the nitrification rate decreased with 35% by changing the set point from 7.5 to
271 6.7, causing TAN accumulation (since the loading rate was higher than the nitrification rate)
272 (SI Section D3 and D4).

273 To obtain a concentrated nitrate rich stream in the middle compartment, the configuration was
274 adapted as further outlined in Section 3.3 and 3.4. Apart from some peaks (e.g., on day 97, 106,
275 152) caused by malfunctioning of the software control system, the pH was stably controlled at
276 a pH of 7.4, resulting in full nitrification in configuration 2 and 3 (effluent TAN and $\text{NO}_2^- \text{-N} <$
277 10 mg N L^{-1} , except on day 141 after a shift to a more concentrated influent batch) (Figure 3A).
278 The OH^- demand for full nitrification was similar to configuration 1 (SI Table S6), since the
279 nitrogen loading rate was stable over time (Table 1). The higher proton concentration in the
280 middle compartment (due to the concentration obtained by the lower influent flow rate to the
281 middle compartment), probably resulted in more proton diffusion over the AEM from the
282 middle compartment to the cathodic compartment in configuration 2 and 3. To compensate for
283 this acidification, more OH^- had to be produced by the electrochemical cell. As a result, a higher
284 current was required to keep the pH at 7.5 compared to configuration 1 (Figure 2B). A higher
285 concentration factor (5 instead of 2) in the middle compartment required a higher OH^-

286 production and current ($235 \text{ mmol OH}^- \text{ L}^{-1} \sim 0.139 \text{ A}$ in configuration 2, concentration factor 5
287 compared to $111 \text{ mmol OH}^- \text{ L}^{-1} \sim 0.062 \text{ A}$ in configuration 2, concentration factor 2). Similar
288 findings were obtained in configuration 3, aiming at both anion and cation extraction and
289 concentration.

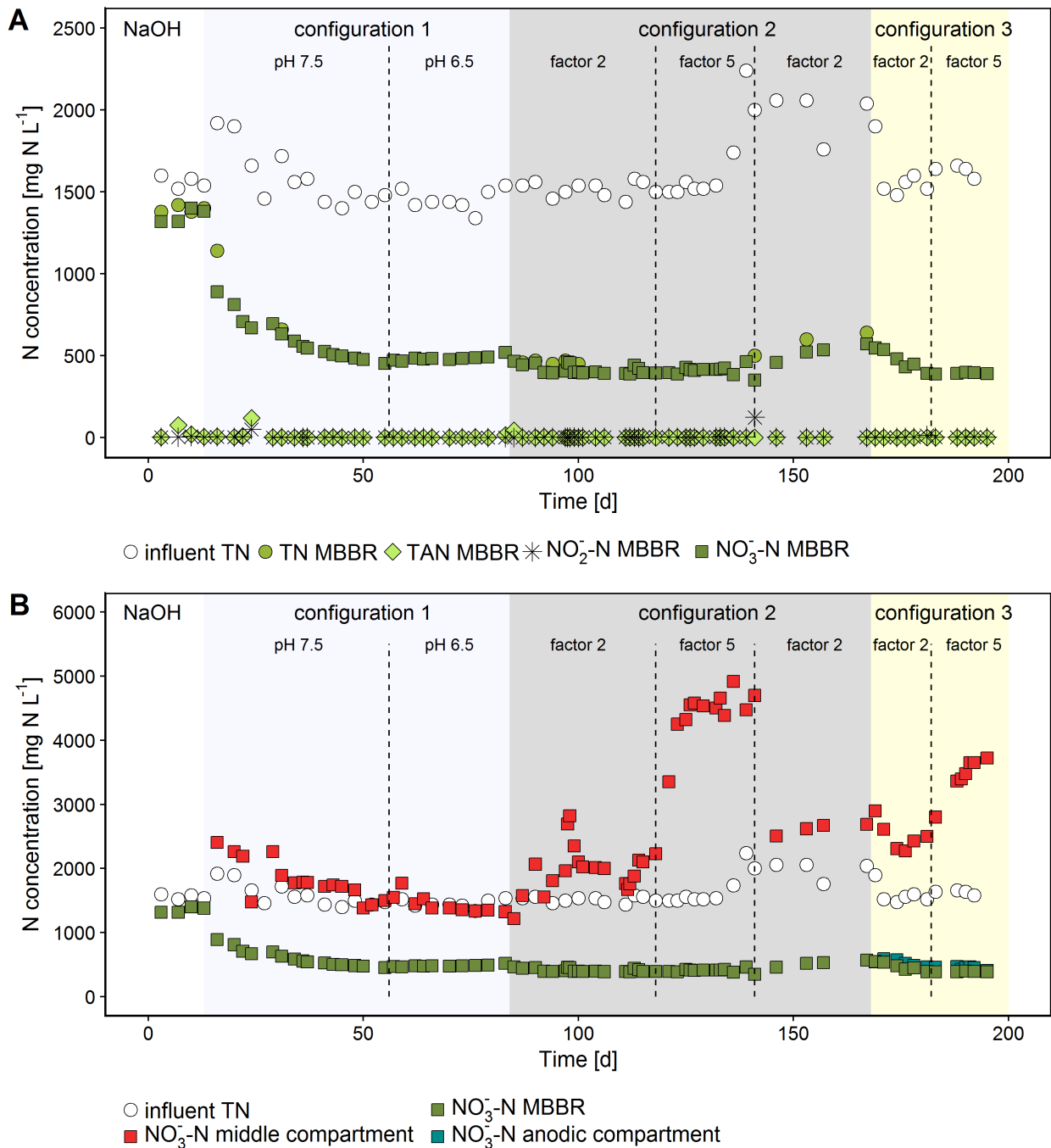
290 Throughout the course of 182 days, the voltage fluctuated between 2.8 and 3.5 V, depending
291 on the current (i.e., a higher current resulted in a higher voltage) (SI Figure S7). The voltage
292 did not display an increasing trend over time, indicating that no or very limited membrane
293 scaling and fouling occurred. The average electrode energy consumption ranged between 7.8
294 kWh m^{-3} or $4.3 \text{ kWh kg}^{-1} \text{ NO}_3^- \text{-N}$ recovered (without concentration in the middle compartment,
295 configuration 1) and 20.9 kWh m^{-3} or $20.5 \text{ kWh kg}^{-1} \text{ NO}_3^- \text{-N}$ recovered (with a concentration
296 factor of 5, configuration 2) (Table S5).

297 **FIGURE 2 - 3**



299

300 **Figure 2. A) pH profile, B) current applied by the electrochemical cell. Averages (AV) and**
 301 **standard deviations (SD) for each operational phase are displayed at the top.**



302

303 **Figure 3. A) total nitrogen (TN) concentration in the influent and TN, TAN, nitrite and**
 304 **nitrate concentration in the effluent, B) TN concentration in the influent and nitrate**
 305 **concentration in the effluent of the bioreactor, middle compartment and anodic**
 306 **compartment.** The average composition of the influent and effluent of the bioreactor, middle
 307 compartment and cathodic compartment are given in SI Tables S1-S4.

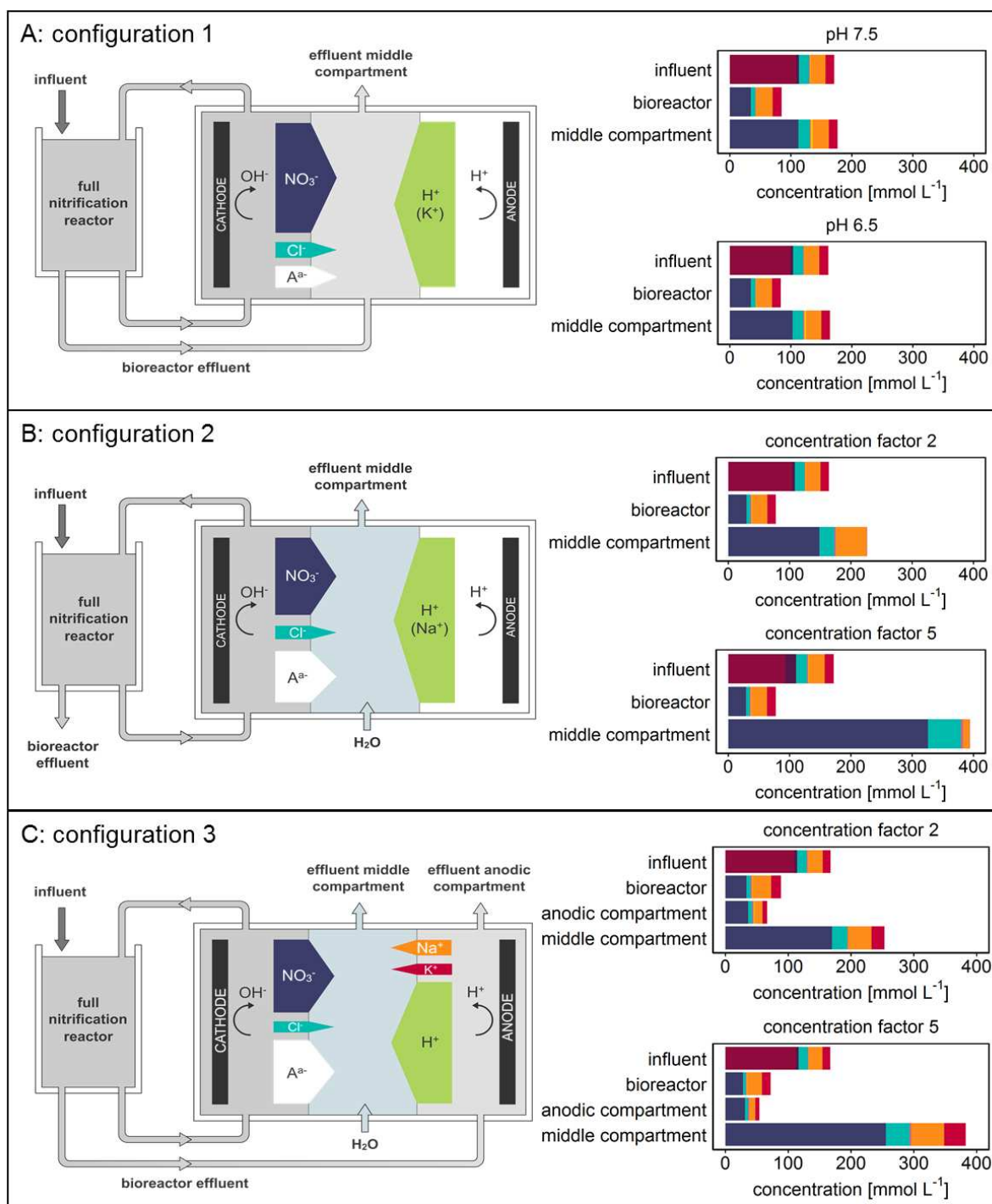
308 **3.2. Configuration 1 enables full nitrate recovery**

309 Due to the electron flow driven by the power supply, anions migrated from the cathodic
310 compartment through the AEM to the middle compartment to restore the charge balance. Nitrate
311 was the predominant anion in the nitrified urine and accounted for an estimated 68-78% of the
312 migration through the AEM in configuration 1 (SI Section B3). Chloride accounted for ~9% of
313 the migration, whereas the contribution of sulfate and phosphate was negligible (<1.5%). The
314 remaining 12-22% can likely be attributed to bicarbonate (was not measured) or hydroxide
315 migration, or to some leakage proton diffusion from the middle compartment (pH<2) to the
316 cathodic compartment. Due to migration, the nitrogen and chloride concentration in the
317 bioreactor were respectively 67-70% and 54-55% lower than the influent concentration, while
318 the concentration of sodium, potassium, phosphate and sulfate did not decrease (Figure 4A,
319 Figure 3A). In order to recover all nitrogen, the effluent from the bioreactor was sent through
320 the middle compartment in configuration 1. The nitrogen and chloride concentration in the
321 effluent of the middle compartment corresponded to the concentration in the influent (Figure
322 3B, SI Tables S1 and S3). Hence, all nitrate and chloride that migrated through the membrane
323 could be captured again in the urine. Evidently, this does not enable creating a concentrate of
324 nitrate.

325 Likewise, the electric field resulted in cation migration from the anodic compartment to the
326 middle compartment (Figure 4A). The anolyte initially consisted of 0.2 M KH_2PO_4 , resulting
327 in proton and potassium migration through the CEM. However, after a few days, potassium was
328 depleted in the anolyte, yielding only proton migration. Due to proton migration, the urine was
329 acidified in the middle compartment (effluent pH<1.5). Assuming that all protons migrated
330 from the anode to the middle compartment, about 100 mmol H^+ L^{-1} was supplied to the middle
331 compartment (based on the current). This was confirmed by means of titrations of the middle

332 compartment effluent, where about 90-115 mmol OH⁻ L⁻¹ was required to increase the pH to
333 6.5-7.5 (SI Figure S8).

334 **FIGURE 4**



335
 336 **Figure 4. Ion migration through the AEM and CEM and composition of the influent,**
 337 **bioreactor liquid, middle compartment and anodic compartment in configuration 1-3. The**
 338 **size of the arrows represent the relative contribution of each ion to the total migration (estimated**
 339 **based on the electric charge) (calculation in SI Section B3). A mass balance is presented in SI,**
 340 **Figure S6.**

341 **3.3. Configuration 2 enables anion extraction and concentration in the middle** 342 **compartment**

343 In configuration 2, nitrate was extracted from the urine and concentrated in the middle
344 compartment, which was fed not with nitrified urine but with demineralized water, yielding a
345 purified acidic nitrate-rich side stream (effluent of the middle compartment) and a nitrate-
346 depleted urine stream (effluent of the bioreactor). Similar to configuration 1, nitrate and protons
347 were the predominant migrating ions through the AEM and CEM, respectively (Figure 4B).
348 Besides protons, sodium migrated from the anolyte (initially 0.2 M Na₂SO₄) through the CEM
349 at an initially high rate. After all sodium was depleted, the sodium concentration in the middle
350 compartment rapidly decreased, as apparent from the difference between the two tested
351 concentration factors (since the anolyte was not replaced when shifting from a concentration
352 factor of 2 to 5). Cation migration from the urine to the middle compartment was mostly
353 prevented by the AEM, and also sulfate and phosphate migration was negligible due to their
354 low concentration. Hence, the effluent from the middle compartment mainly consisted of nitrate
355 ($2.1 \pm 0.3 \text{ g NO}_3^- \text{-N L}^{-1}$ at factor 2 and $4.6 \pm 0.2 \text{ g NO}_3^- \text{-N L}^{-1}$ at factor 5), chloride ($0.9 \pm 0.2 \text{ g}$
356 $\text{Cl}^- \text{ L}^{-1}$ at factor 2 and $1.9 \pm 0.2 \text{ g Cl}^- \text{ L}^{-1}$ at factor 5), and sodium (originating from the anolyte)
357 in an aqueous matrix with a pH below 1.2 (Figure 4B, SI Table S3). This is in contrast to
358 configuration 1, where only one effluent stream, derived from the middle compartment, with a
359 composition and matrix similar to the influent was obtained (only urea was converted into
360 nitrate and COD was removed). While most pathogens and micropollutants are retained by the
361 ion exchange membrane²⁵⁻²⁷, these urine originating contaminants can be re-introduced in the
362 effluent of configuration 1 by redirecting the bioreactor content to the middle compartment.
363 This as opposed to configuration 2, where a contaminant-free aqueous end product is obtained,
364 although in depth analysis would be necessary to fully confirm this.

365 About 30% of the nitrate remained in the urine and was not recovered in the middle
366 compartment. As anion migration restores the charge balance by compensating for the
367 production of negatively charged OH^- ions, the extent of nitrate migration is limited by the OH^-
368 demand, which in turn depends on the nitrogen load. Hence, the nitrate recovery could be
369 increased by increasing the OH^- demand in the bioreactor. The latter could be achieved by
370 eliminating the electrochemical alkalization pre-treatment (which provided 11-22% of the
371 OH^- , SI Table S6). However, given the discontinuous nature of urine supplies, the high
372 variability in composition and the fact that nitrifiers are very susceptible to peak loadings,
373 storage in an equalization tank is important in order to provide a constant influent flow and
374 loading to the bioreactor. Eliminating or minimizing the OH^- addition in the electrochemical
375 pre-treatment would result in a $\text{pH} < 12$, thereby increasing the risk for urea hydrolysis during
376 storage. In De Paepe et al. (2020)⁶, increasing the pH to 11 was insufficient to prevent urea
377 hydrolysis for longer than one week. Moreover, no or less chloride would be removed by the
378 electrochemical pre-treatment, increasing the competition between nitrate and chloride for
379 migration in the electrochemical cell of the bioreactor. Alternatively, the OH^- demand could be
380 increased by redirecting a part of the anolyte to the bioreactor. This would result in an
381 acidification of the bioreactor, and, a concurrent increase of the OH^- demand, at the expense of
382 a higher energy consumption. A third option to improve the nitrate recovery, is the use of an
383 AEM with a high nitrate to chloride selectivity in order to favor nitrate migration. The
384 chloride/nitrogen ratio in the middle compartment corresponded to the ratio of the influent,
385 indicating that the monovalent AEM used in this study had the same selectivity for nitrate and
386 chloride. Membranes with a nitrate to chloride selectivity of 2²⁸ to 4.68²⁹ have been developed.
387 A fourth option to improve the nitrate recovery is the use of a cell with multiple AEM and CEM
388 cell pairs, which enables to uncouple the nitrate migration from the OH^- demand.

389 In addition to extraction, concentration was achieved in the middle compartment by minimizing
390 the influent (water) flow, thereby capturing the nutrients in a smaller volume. In a first phase,
391 with an influent flow rate of 223 mL H₂O d⁻¹ to the middle compartment (Q_{in} bioreactor/ Q_{in}
392 middle compartment~2), the nitrate concentration was about 1.3 times higher compared to the
393 total nitrogen concentration in the influent of the MBBR. By further decreasing the influent
394 water flow rate to 94 ± 4 mL d⁻¹ (Q_{in} bioreactor/ Q_{in} middle compartment~5), this value increased
395 to 3. As for nitrate, protons were more concentrated at factor 5 (pH of 0.7 ± 0.1 compared to
396 1.1 ± 0.1 at factor 2) (SI Figure S9). The discrepancy between the theoretical concentration
397 factor (~2 and ~5) and the actual nitrate concentration factor (1.3 and 3) is due to incomplete
398 nitrate recovery (i.e., 30% remained in urine). Osmotic and electro-osmotic water transport
399 became more substantial with an increasing concentration factor because of the increased
400 concentration gradient and ion migration. In case of factor 5, with an influent water flow rate
401 of 94 mL d⁻¹, the effluent flow rate of the middle compartment amounted to 120 mL d⁻¹,
402 corresponding to an influent ratio (Q_{in} bioreactor/ Q_{in} middle compartment) of 5.7 and an
403 effluent ratio (Q_{in} bioreactor/ Q_{out} middle compartment) of only 4.5. This presents limits to the
404 maximum achievable concentration in the middle compartment. Furthermore, the energy
405 consumption increases with the concentration factor. Three times more energy was required for
406 a factor 5 concentration compared to configuration 1 without concentration (SI Table S5).

407 **TABLE 2**

408 **Table 2. Overview of concentration factors and nitrogen recovery in configuration 2 and**
 409 **3.**

Concentration factor	Configuration 2		Configuration 3	
	2	5	2	5
$\frac{Q_{in} \text{ bioreactor}}{Q_{in} \text{ middle compartment}}$	2.2	5.7	2.5	5.3
$\frac{Q_{in} \text{ bioreactor}}{Q_{out} \text{ middle compartment}}$	2.2	4.5	2.2	3.8
$\frac{[NO_3^- - N] \text{ middle compartment}}{[TN] \text{ influent}}$	1.3	3.0	1.5	2.3
Nitrogen recovery				
$1 - \frac{[NO_3^- - N] \text{ bioreactor}}{[TN] \text{ influent}}$	73	74	70-73	76

410

411 **3.4. Configuration 3 enables anion and cation extraction and concentration in the middle**
 412 **compartment**

413 In configuration 2, all cations were retained in the urine. In order to recover part of the
 414 potassium (which is an important plant nutrient), the effluent of the bioreactor was sent through
 415 the anodic compartment in configuration 3. As a result, besides protons produced at the anode,
 416 also sodium and potassium from the urine migrated through the CEM to the middle
 417 compartment, accounting for an estimated 8-11% and 4-6% of the migration, respectively
 418 (Figure 4C, SI Section B3). This resulted in a recovery of on average 40% of the potassium and
 419 44% of the sodium from urine.

420 Anion migration through the AEM was identical to configuration 2, meaning that ~30% of the
 421 nitrate and ~40% of the chloride remained in the urine. As a consequence, by diverting the
 422 effluent of the bioreactor to the anodic compartment, chloride entered the anodic compartment,
 423 where it could be oxidized at the anode to chlorine, which could diffuse to the atmosphere
 424 (chlorine gas is toxic) or further react to HOCl, a known disinfectant, or undesired disinfection

425 by-products such as organochlorides and chlorate (ClO_3^-)³⁰. If HOCl were to diffuse to the
426 bioreactor, it could inactivate or kill the microbial community, hampering nitrification and
427 COD oxidation. The latter was not observed, indicating that configuration 3 is a promising
428 alternative to configuration 2, offering the advantage of both anion and cation recovery. As
429 HOCl decreases the lifespan of most membranes, a HOCl resistant CEM might be required for
430 long-term operation.

431 No major differences were observed with respect to the concentration effects. In line with
432 configuration 2, a 5 times concentration factor showed a higher concentration of nitrate, a lower
433 pH in the middle compartment, more osmotic and electro-osmotic water transport, and a higher
434 energy consumption compared to a concentration factor of 2.

435 **3.5 COD removal eliminates the risk for downstream biofouling**

436 Besides nitrification, COD was converted into CO_2 and biomass by heterotrophic bacteria in
437 the bioreactor. In all reactors, throughout all operational phases, 82-95% of the COD was
438 removed, which is in line with typical COD removal percentages by open communities reported
439 in literature (SI Tables S1, S2, S10, S11 and S13).^{7, 10, 11, 14, 31-33} The COD removal percentage
440 was not affected by the pH set point in configuration 1 or by the concentration factor in
441 configuration 2 and 3. Since all rapidly biodegradable COD was removed, the risk for
442 downstream biofouling was likely eliminated.

443 **3.6. Electrochemical pH control offers competitive benefits compared to partial** 444 **nitrification and full nitrification with base addition**

445 To compare the novel electrochemical pH control strategy with more common approaches such
446 as base addition or partial nitrification, an identical MBBR with NaOH addition and an MBBR
447 without pH control were operated (SI Section C and D).

448 Due to a lack of alkalinity, partial nitrification was obtained in the MBBR without pH control.
449 In a first phase, with an influent pH of 11.9 ± 0.2 , about 40% of the nitrogen in the effluent
450 consisted of TAN, whereas ~60% was nitrified to nitrate (SI Section C3). This NO_3^- -N/TAN
451 ratio (60:40) is higher than reported in literature (typically ~50:50^{11, 32, 34}), because of the OH^-
452 addition for alkalization (SI Table S12). In an attempt to increase the NO_3^- -N/TAN ratio,
453 influent with a higher alkalinity was fed to the reactor. Although the NO_3^- -N/TAN could be
454 increased via the influent alkalinity (SI Section C3), it proved difficult to regulate since the OH^-
455 demand depends on the nitrogen concentration in urine, which highly fluctuates.

456 Similar to the reactor with electrochemical pH control, full nitrification was obtained in the
457 MBBR with NaOH addition (SI Section D). The salinity of the reactor with NaOH addition was
458 however markedly higher compared to the salinity of the middle compartment effluent in
459 configuration 1 (SI Section E). This is on the one hand due to the upstream electrochemical
460 alkalization (to pH 12), which reduced the concentration of chloride (and other anions) in the
461 influent of the MBBR with electrochemical OH^- addition with more than 60% compared to the
462 NaOH-alkalinized influent used to feed the MBBR with NaOH addition (Section 2.2). On the
463 other hand, sodium addition (originating from the use of NaOH for alkalization and full
464 nitrification) increased the sodium concentration fivefold compared to the original
465 concentration in urine (before alkalization) in the MBBR with NaOH addition, whereas no
466 sodium was dosed to the MBBR with electrochemical OH^- addition. An additional advantage
467 of the electrochemical pH control is that the nitrifiers in the bioreactor are exposed to an even
468 lower salinity because of anion migration to the middle compartment (which decreased the
469 chloride and nitrate concentration in the bioreactor with 55-70%). This is particularly relevant
470 when working with salt-sensitive synthetic communities in high strength urine.¹³

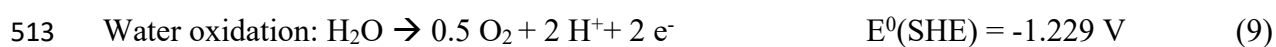
471 A preliminary cost comparison (SI Table S16) showed that the energy cost for electrochemical
472 pH control (€3.8-9.0 m⁻³ urine) is in the same range as the cost of NaOH addition (€3.2 m⁻³
473 urine).

474 **3.7 Application of electrochemical in-situ pH control and extraction**

475 In this study, we showed that coupling of a urine nitrification bioreactor with an electrochemical
476 system can provide a convenient and innovative alternative to base addition, enabling full
477 nitrification while avoiding the use of chemicals (bases), the logistics associated with base
478 storage and dosing, and the associated increase in salinity. Furthermore, the electrochemical
479 cell can flexibly be integrated with the nitrification reactor, and each resulting configuration
480 has its own benefits and application potential. When full nitrogen recovery is sought and further
481 nitrogen concentration/refinery is not important, configuration 1 proved to be the better option.
482 All urine compounds, including macronutrients and trace elements (except organics and the
483 phosphorus, calcium and magnesium precipitated in the alkalization step) are then recovered
484 in the nitrified urine. The urine precipitates could be redissolved in the acidic nitrified urine. In
485 contrast, configurations 2 and 3 each yielded two streams, i.e., a purified concentrated acidic
486 nitrate-rich product stream and a nitrate-depleted treated urine effluent (SI Figure S16). These
487 configurations result in a lower nitrate recovery but are particularly valuable when interested in
488 a refined and concentrated end product, which facilitates storage and transport. Only a limited
489 number of compounds is recovered in the concentrated stream, which can be an advantage (if
490 only nitrate recovery is targeted) or a disadvantage (since other macronutrients and trace
491 elements are lost). Important in this respect is that configuration 3 allows to recover more
492 compounds, including potassium, an important fertilizer constituent. The concentration factors
493 fall within the same range as those obtained by electrodialysis^{7,35,36}, while the electrode energy
494 consumption is higher (25-60 kWh electrical energy or 75-200 kWh primary energy m⁻³ urine
495 compared to only 4.4 kWh electrical energy m⁻³ urine with electrodialysis⁷) (SI Table S5).

496 Additionally, both methods consume energy for pumping. Distillation reaches higher
497 concentration factors but at the expense of a higher energy investment (~700 kWh primary
498 energy m⁻³ urine).¹⁴

499 Besides hydroxide ions or protons, hydrogen gas (25-62 mmol H₂ d⁻¹) and oxygen gas (12-31
500 mmol O₂ d⁻¹) were produced by water reduction and water oxidation at the cathode and anode,
501 respectively. Redirecting the oxygen gas to the bioreactor could cover 10-25% of the theoretical
502 oxygen demand for nitrification and COD oxidation (assuming an oxygen demand of 4.33 g O₂
503 g⁻¹ N nitrified and 0.8 g O₂ g⁻¹ COD removed). Alternatively, recycling of the cathodically
504 generated hydrogen gas to the anode could shift the anode reaction from water oxidation to
505 hydrogen gas oxidation, thereby decreasing the anode potential and thus the energy
506 consumption by the electrochemical cell, as demonstrated by Kuntke et al. in a TAN recovery
507 electrochemical system.^{37, 38} This implies that a gas stream (containing hydrogen gas) is
508 recirculated over the anodic compartment (containing a gas diffusion electrode) instead of a
509 liquid stream (anolyte solution). This is not compatible with configuration 3, since the
510 bioreactor effluent is redirected over the anodic compartment. In configuration 1 and 2 on the
511 contrary, it can be implemented, but requires additional stripping of the hydrogen gas from the
512 bioreactor liquid at the exit of the cathodic compartment.



515 The technology is mainly suited for small decentralized urine treatment systems. The
516 electrochemical cell connected to the bioreactor (3.5 L) had a size of 100 cm² and was operated
517 at a current density of 0-20 A m⁻², which is low (current density can be increased up to ~100 A
518 m⁻² or higher). Hence, for a bioreactor of 35 L, the same electrochemical cell could have been
519 used. For larger reactors, the size of the electrochemical cell can be increased or multiple units

520 can be operated in parallel. The main limitation is however the fact that the bioreactor liquid
521 has to be recirculated over the cathode. Recirculation is rather uncommon in large scale
522 bioreactors in practice.

523 Urine treatment and recycling are not only relevant on Earth, but are of major importance in
524 regenerative life support systems (RLSS) as urine is the main resource of water and nutrients.
525 Even when recovery is not envisaged, urine stabilization is essential since ammonia, originating
526 from urea hydrolysis, can pose a hazard to the crew upon volatilization. Currently, on board of
527 the International Space Station, sulfuric/phosphoric acid and toxic chromium trioxide are added
528 to urine in order to inhibit urea hydrolysis.³⁹ Subsequently, water is recovered from the urine
529 using vapor compression distillation and filtration, while the nutrients are concentrated in a
530 toxic brine.⁴⁰ Alternatively, urine could be stabilized by the two-step approach presented in
531 this study. Immediately after collection, the pH should be increased to 12 in order to prevent
532 urea hydrolysis during storage, which is essential to provide a constant flow and composition
533 to the bioreactor, where all urea is nitrified to nitrate. The nitrified urine can be valorized as
534 substrate for plants and microalgae. Nitrification combined with the production of microalgae
535 and plants is being explored in the framework of the Micro-Ecological Life Support System
536 Alternative (MELiSSA), the RLSS programme from the European Space Agency.^{13, 41} To take
537 this one step further, this study addressed the issue of payload limitations to Space by
538 implementation of electrochemical cells enabling in-situ production of acids and bases,
539 obviating the need for transportation and storage of these hazardous consumables.
540 Configuration 1 is most appropriate for Space application as maximum recovery is pivotal while
541 concentration does not present an added value in Space. Furthermore, the low salinity and
542 acidity ($\sim 1 \text{ mol H}^+ \text{ mol}^{-1} \text{ NO}_3^- \text{-N}$) of the end product of configuration 1 are compatible with
543 hydroponic plant production, as $0\text{-}1 \text{ mol H}^+ \text{ mol}^{-1} \text{ NO}_3^- \text{-N}$ is required to compensate for the
544 release of OH^- ions ($0\text{-}1 \text{ mol OH}^- \text{ mol}^{-1} \text{ NO}_3^- \text{-N}$) that accompanies nitrate uptake by most

545 plants.^{18, 42, 43} The low pH is furthermore well suited for dissolving the urine precipitates formed
546 in the alkalization step, which would increase the phosphate content and the pH of the end-
547 product. For other applications (e.g., microalgae cultivation), further neutralization might be
548 required. This could be achieved by adapting the configuration (e.g., by sending another waste
549 stream through the anodic compartment) or by using another electrochemical cell to avoid the
550 use of chemicals.

551 ASSOCIATED CONTENT

552 **Supporting Information.** The Supporting Information is available free of charge at: ...

553 Experimental setup and operation; additional tables and figures of the full nitrification
554 reactor with electrochemical hydroxide addition (composition of influent, bioreactor
555 effluent, middle compartment effluent and anodic compartment effluent,
556 electrochemical hydroxide production and energy consumption, electromigration),
557 material and methods and results of the partial nitrification reactor without pH control
558 and of the full nitrification reactor with NaOH addition; Comparison of the three pH
559 control strategies (salinity and cost).

560 AUTHOR INFORMATION

561 **Corresponding Author**

562 *E-mail: Korneel.Rabaey@UGent.be

563 **Notes**

564 The authors declare no competing financial interest

565 ACKNOWLEDGMENT

566 This article has been made possible through the authors' involvement in the MELiSSA
567 project, the life support system research program from the European Space Agency (ESA)
568 (<https://www.melissafoundation.org/>).

569 The authors would like to acknowledge

570 i) the MELiSSA foundation to support JDP via the POMP1 (Pool Of MELiSSA PhD)
571 program,

572 ii) the Research Foundation Flanders to support KR (FWO microelectronics G.0206.16 N.),

- 573 iii) the Belgian Science Policy (BELSPO) to support RG via the URINIS-A phase 2 project,
- 574 iv) Avecom for providing ABIL sludge,
- 575 v) Mike Taghon and Annick Beyaert for making the LabVIEW control system,
- 576 vi) Kim De Paepe for critically reviewing the manuscript.

577 REFERENCES

- 578 1. Maurer, M.; Pronk, W.; Larsen, T. A., Treatment processes for source-separated urine. *Water*
579 *Res.* **2006**, *40*, (17), 3151-3166.
- 580 2. National Research Council (US), *Committee on Acute Exposure Guideline Levels. Acute*
581 *Exposure Guideline Levels for Selected Airborne Chemicals: Volume 6. Washington (DC): National*
582 *Academies Press (US); 2008. 2, Ammonia Acute Exposure Guideline Levels. Available from:*
583 <https://www.ncbi.nlm.nih.gov/books/NBK207883/>. 2008.
- 584 3. Udert, K. M.; Larsen, T. A.; Biebow, M.; Gujer, W., Urea hydrolysis and precipitation dynamics
585 in a urine-collecting system. *Water Res.* **2003**, *37*, (11), 2571-2582.
- 586 4. Udert, K. M.; Larsen, T. A.; Gujer, W., Fate of major compounds in source-separated urine.
587 *Water Sci. Technol.* **2006**, *54*, (11-12), 413-420.
- 588 5. Chipako, T. L.; Randall, D. G., Urine treatment technologies and the importance of pH. *J.*
589 *Environ. Chem. Eng.* **2020**, *8*, (1), 103622.
- 590 6. De Paepe, J.; De Pryck, L.; Verliefe, A. R. D.; Rabaey, K.; Clauwaert, P., Electrochemically
591 Induced Precipitation Enables Fresh Urine Stabilization and Facilitates Source Separation. *Environ.*
592 *Sci. Technol.* **2020**, *54*, (6), 3618-3627.
- 593 7. De Paepe, J.; Lindeboom, R. E. F.; Vanoppen, M.; De Paepe, K.; Demey, D.; Coessens, W.;
594 Lamaze, B.; Verliefe, A. R. D.; Clauwaert, P.; Vlaeminck, S. E., Refinery and concentration of
595 nutrients from urine with electro dialysis enabled by upstream precipitation and nitrification. *Water*
596 *Res.* **2018**, *144*, 76-86.
- 597 8. Randall, D. G.; Krahenbuhl, M.; Kopping, I.; Larsen, T. A.; Udert, K. M., A novel approach for
598 stabilizing fresh urine by calcium hydroxide addition. *Water Res.* **2016**, *95*, 361-369.
- 599 9. Senecal, J.; Vinneras, B., Urea stabilisation and concentration for urine-diverting dry toilets:
600 Urine dehydration in ash. *Sci Total Environ* **2017**, *586*, 650-657.
- 601 10. Coppens, J.; Lindeboom, R.; Muys, M.; Coessens, W.; Alloul, A.; Meerbergen, K.; Lievens, B.;
602 Clauwaert, P.; Boon, N.; Vlaeminck, S. E., Nitrification and microalgae cultivation for two-stage
603 biological nutrient valorization from source separated urine. *Bioresour. Technol.* **2016**, *211*, 41-50.
- 604 11. Udert, K. M.; Fux, C.; Munster, M.; Larsen, T. A.; Siegrist, H.; Gujer, W., Nitrification and
605 autotrophic denitrification of source-separated urine. *Water Sci. Technol.* **2003**, *48*, (1), 119-130.
- 606 12. Feng, D. L.; Wu, Z. C.; Xu, S. H., Nitrification of human urine for its stabilization and nutrient
607 recycling. *Bioresour. Technol.* **2008**, *99*, (14), 6299-6304.
- 608 13. Christiaens, M. E. R.; De Paepe, J.; Ilgrande, C.; De Vrieze, J.; Barys, J.; Teirlinck, P.;
609 Meerbergen, K.; Lievens, B.; Boon, N.; Clauwaert, P.; Vlaeminck, S. E., Urine nitrification with a
610 synthetic microbial community. *Systematic and Applied Microbiology* **2019**, 126021.
- 611 14. Udert, K. M.; Wachter, M., Complete nutrient recovery from source-separated urine by
612 nitrification and distillation. *Water Res.* **2012**, *46*, (2), 453-464.
- 613 15. Fumasoli, A.; Etter, B.; Sterkele, B.; Morgenroth, E.; Udert, K. M., Operating a pilot-scale
614 nitrification/distillation plant for complete nutrient recovery from urine. *Water Sci. Technol.* **2016**,
615 *73*, (1), 215-222.
- 616 16. Parida, A. K.; Das, A. B., Salt tolerance and salinity effects on plants: a review. *Ecotoxicology*
617 *and Environmental Safety* **2005**, *60*, (3), 324-349.
- 618 17. Munns, R.; Tester, M., Mechanisms of salinity tolerance. *Annual review of plant biology* **2008**,
619 *59*, 651-81.
- 620 18. Spinu, V. C.; Langhans, R. W.; Albright, L. D. In *ELECTROCHEMICAL PH CONTROL IN*
621 *HYDROPONIC SYSTEMS*, 1998; International Society for Horticultural Science (ISHS), Leuven, Belgium:
622 1998; pp 275-282.
- 623 19. Schwartzkopf, S. H. *Electrochemical Control of pH in a Hydroponic Nutrient Solution. Available*
624 *at: <https://ntrs.nasa.gov/archive/nasa/casi.ntrs.nasa.gov/19860010447.pdf>; 1986.*

- 625 20. Walther, I.; van der Schoot, B. H.; Jeanneret, S.; Arquint, P.; de Rooij, N. F.; Gass, V.; Bechler,
626 B.; Lorenzi, G.; Cogoli, A., Development of a miniature bioreactor for continuous culture in a space
627 laboratory. *Journal of Biotechnology* **1994**, *38*, (1), 21-32.
- 628 21. Andersen, S. J.; Candry, P.; Basadre, T.; Khor, W. C.; Roume, H.; Hernandez-Sanabria, E.;
629 Coma, M.; Rabaey, K., Electrolytic extraction drives volatile fatty acid chain elongation through lactic
630 acid and replaces chemical pH control in thin stillage fermentation. *Biotechnology for Biofuels* **2015**,
631 *8*, (1), 221.
- 632 22. Bonvin, C.; Etter, B.; Udert, K. M.; Frossard, E.; Nanzer, S.; Tamburini, F.; Oberson, A., Plant
633 uptake of phosphorus and nitrogen recycled from synthetic source-separated urine. *Ambio* **2015**, *44*,
634 S217-S227.
- 635 23. Muys, M.; Coppens, J.; Boon, N.; Vlaeminck, S. E., Photosynthetic oxygenation for urine
636 nitrification. *Water Sci. Technol.* **2018**, *78*, (1), 183-194.
- 637 24. Wohlsager, S.; Clemens, J.; Nguyet, P. T.; Rechenburg, A.; Arnold, U., Urine--a valuable
638 fertilizer with low risk after storage in the tropics. *Water environment research : a research
639 publication of the Water Environment Federation* **2010**, *82*, (9), 840-7.
- 640 25. Escher, B. I.; Pronk, W.; Suter, M. J. F.; Maurer, M., Monitoring the removal efficiency of
641 pharmaceuticals and hormones in different treatment processes of source-separated urine with
642 bioassays. *Environ. Sci. Technol.* **2006**, *40*, (16), 5095-5101.
- 643 26. Pronk, W.; Kone, D., Options for urine treatment in developing countries. *Desalination* **2009**,
644 *248*, (1-3), 360-368.
- 645 27. Pronk, W.; Biebow, M.; Boller, P., Treatment of source-separated urine by a combination of
646 bipolar electrodialysis and a gas transfer membrane. *Water Sci. Technol.* **2006**, *53*, (3), 139-146.
- 647 28. Eyal, A.; Kedem, O., Nitrate-selective anion-exchange membranes. *J. Membr. Sci.* **1988**, *38*,
648 (2), 101-111.
- 649 29. Kikhavani, T.; Ashrafizadeh, S. N.; Van der Bruggen, B., Nitrate Selectivity and Transport
650 Properties of a Novel Anion Exchange Membrane in Electrodialysis. *Electrochimica Acta* **2014**, *144*,
651 341-351.
- 652 30. Jung, Y. J.; Baek, K. W.; Oh, B. S.; Kang, J.-W., An investigation of the formation of chlorate
653 and perchlorate during electrolysis using Pt/Ti electrodes: The effects of pH and reactive oxygen
654 species and the results of kinetic studies. *Water Res.* **2010**, *44*, (18), 5345-5355.
- 655 31. Jiang, F.; Chen, Y.; Mackey, H. R.; Chen, G. H.; van Loosdrecht, M. C. M., Urine nitrification
656 and sewer discharge to realize in-sewer denitrification to simplify sewage treatment in Hong Kong.
657 *Water Sci. Technol.* **2011**, *64*, (3), 618-626.
- 658 32. Bischel, H. N.; Schertenleib, A.; Fumasoli, A.; Udert, K. M.; Kohn, T., Inactivation kinetics and
659 mechanisms of viral and bacterial pathogen surrogates during urine nitrification. *Environ. Sci.-Wat.
660 Res. Technol.* **2015**, *1*, (1), 65-76.
- 661 33. Chen, L. P.; Yang, X. X.; Tian, X. J.; Yao, S.; Li, J. Y.; Wang, A. M.; Yao, Q. A.; Peng, D. C., Partial
662 nitritation of stored source-separated urine by granular activated sludge in a sequencing batch
663 reactor. *AMB Express* **2017**, *7*, 1-10.
- 664 34. Feng, D. L.; Wu, Z. C.; Wang, D. H., Effects of N source and nitrification pretreatment on
665 growth of *Arthrospira platensis* in human urine. *J. Zhejiang Univ.-SCI A* **2007**, *8*, (11), 1846-1852.
- 666 35. Pronk, W.; Zuleeg, S.; Lienert, J.; Escher, B.; Koller, M.; Berner, A.; Koch, G.; Boller, M., Pilot
667 experiments with electrodialysis and ozonation for the production of a fertiliser from urine. *Water
668 Sci. Technol.* **2007**, *56*, (5), 219-227.
- 669 36. Pronk, W.; Biebow, M.; Boller, M., Electrodialysis for recovering salts from a urine solution
670 containing micropollutants. *Environ. Sci. Technol.* **2006**, *40*, (7), 2414-2420.
- 671 37. Kuntke, P.; Rodríguez Arredondo, M.; Widyakristi, L.; ter Heijne, A.; Sleutels, T. H. J. A.;
672 Hamelers, H. V. M.; Buisman, C. J. N., Hydrogen Gas Recycling for Energy Efficient Ammonia Recovery
673 in Electrochemical Systems. *Environ. Sci. Technol.* **2017**, *51*, (5), 3110-3116.
- 674 38. Kuntke, P.; Rodrigues, M.; Sleutels, T.; Saakes, M.; Hamelers, H. V. M.; Buisman, C. J. N.,
675 Energy-Efficient Ammonia Recovery in an Up-Scaled Hydrogen Gas Recycling Electrochemical System.
676 *ACS Sustainable Chemistry & Engineering* **2018**, *6*, (6), 7638-7644.

- 677 39. Muirhead, D.; Carter, D. L.; Williamson, J., Preventing Precipitation in the ISS Urine Processor
678 In *48th International Conference on Environmental Systems*, Albuquerque, New Mexico, 2018.
- 679 40. Carter, D. L.; Williamson, J.; Brown, C. A.; Bazley, J.; Gazda, D.; Schaezler, R.; THomas, F.,
680 Status of ISS Water Management and Recovery. In *48th International Conference on Environmental*
681 *Systems*, Albuquerque, New Mexico, 2017.
- 682 41. Gòdia, F.; Albiol, J.; Montesinos, J. L.; Pérez, J.; Creus, N.; Cabello, F.; Mengual, X.; Montras,
683 A.; Lasseur, C., MELISSA: a loop of interconnected bioreactors to develop life support in Space.
684 *Journal of Biotechnology* **2002**, *99*, (3), 319-330.
- 685 42. FAN, X. H.; TANG, C.; RENGEL, Z., Nitrate Uptake, Nitrate Reductase Distribution and their
686 Relation to Proton Release in Five Nodulated Grain Legumes. *Annals of Botany* **2002**, *90*, (3), 315-323.
- 687 43. Bolan, N. S.; Hedley, M. J.; White, R. E., Processes of soil acidification during nitrogen cycling
688 with emphasis on legume based pastures. *Plant and Soil* **1991**, *134*, (1), 53-63.

689